



**VISHAY**  
**PRECISION**  
**GROUP**

# **PhotoStress®**

## **Micro-Measurements**

- **A Brief Introduction**
- **Pictorial Examples of—**
  - **PhotoStress-Coated Parts**
  - **A Wide Selection of Industrial Case History Applications**



[www.photostress.com](http://www.photostress.com)

# Introduction to PhotoStress

PhotoStress is a widely used full-field technique for accurately measuring surface strains to determine the stresses in a part or structure during static or dynamic testing.

With the PhotoStress method, a special strain-sensitive plastic coating is first bonded to the test part. Then, as test or service loads are applied to the part, the strains on the surface of the part are transmitted to the coating which assumes the same strain condition as the part. The coating is then illuminated by polarized light from a reflection polariscope. When viewed through the polariscope, the coating



Fig. 1—PhotoStress pattern revealed on a mechanical controlled linkage system in a passenger jet aircraft.

displays the strains (or stresses) in a colorful, informative pattern (Fig. 1), which immediately reveals the overall stress distribution and pinpoints highly stressed areas. With an optical transducer (digital compensator) attached to the polariscope, quantitative stress analysis can be quickly and easily performed. Permanent records of the overall stress distribution can be made by photography or by video recording.

PhotoStress offers the following types of analysis and measurements:

1. Full-field analysis, permitting overall assessment of strain/stress magnitudes and gradients, and areas of maximum stress.
2. Quantitative measurements expressed in stress units (psi) or in strain units ( $\text{in/in} \times 10^{-6}$ ):
  - a. The directions of principal stresses at all points on the surface of the structure.
  - b. The magnitude and sign of the tangential stress along free boundaries, and in all regions where the state of stress is uniaxial.
  - c. In a biaxial stress state, the magnitude of the difference in principal stresses at any selected point on the coated surface of the test object.
  - d. Individual values and sign of principal stresses by the PhotoStress slitting method.

Special Features:

- Immediate recognition of stress gradients and overall stress distribution.
- Immediate identification of overstressed and understressed areas.
- Observation of stress distribution under varying modes of loading.
- Comparison between the actual stress distribution obtained by PhotoStress analysis and the modeling analysis by Finite Element (FEA). This leads to better understanding of FEA.
- Areas of yielding (elastoplastic deformations) can be identified and measured after the part is unloaded, by observing and measuring the residual color pattern.

### FULL-FIELD INTERPRETATION OF STRESS DISTRIBUTION

The photoelastic strain pattern appears as a series of successive and contiguous different colored bands (isochromatics) in which each band represents a different degree of magnitude of the difference in principal stresses ( $\sigma_1 - \sigma_2$ ). Initially at no-load condition, the coated part appears black (no color). When load is applied gradually, first colors appear in areas of highest stress. When load continues to increase, color bands spread throughout the part. A trained technician can at that time determine areas of zero stress, stress gradients, and overall stress distribution. Figure 2 illustrates this color change sequence (from left to right) on a PhotoStress-coated aluminum sample subjected to increasing tensile load levels.

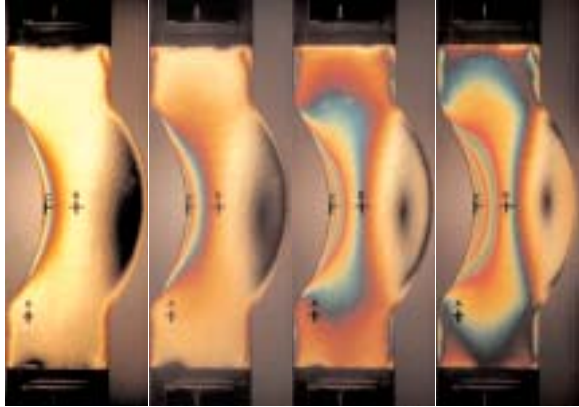


Fig. 2

Figure 2 illustrates this color change sequence (from left to right) on a PhotoStress-coated aluminum sample subjected to increasing tensile load levels.

### MEASUREMENTS OF STRESSES AT A POINT

Colors may be identified as stress values; however, to obtain quantitative measurements, a measuring device (compensator) should be used. The measurement is done by turning a dial of the compensator until the colors disappear at the point of measurement (see Fig. 3). The number indicated on the compensator is then translated to stresses by a computer using the PhotoStress PSCalc™ software.



Fig. 3

To measure the directions of principal stresses, another dial is turned until a black line covers the point of measurement (see Fig. 4). Directions of principal stresses are then indicated on the structure by a laser light.

Using the above simple procedure, maximum stress ( $\sigma_1$ ) as well as the difference in principal stress ( $\sigma_1 - \sigma_2$ ) are obtainable.

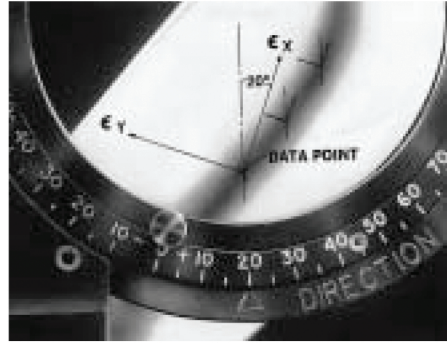


Fig. 4

**Note 1:** The PhotoStress coating is a strain sensitive material, and the measurement is actually of strain. Through the use of the structure's mechanical properties the strains are converted to stresses.

**Note 2:** For complete information on the theory of PhotoStress, coating of parts, and the measurement process in detail, see Vishay Precision Group Tech Note TN-702, "Introduction to Stress Analysis by the PhotoStress® Method" (VMM-TN0702).

# Examples of PhotoStress-Coated Parts

PhotoStress coatings can be applied to the surface of virtually any test part regardless of its shape, size, or material composition. For coating complex shapes, liquid plastic is cast on a flat-plate mold and allowed to partially polymerize. While still in a pliable state, the sheet is removed from the mold and formed by hand to the contours of the test part (shown below). When fully cured, the plastic coating is bonded in place with special reflective cement, and the part is then ready for testing. For plane surfaces, premanufactured flat sheets are cut to size and bonded directly to the test part.

The following pages show typical PhotoStress-coated parts for testing.



PhotoStress coating being contoured to the surface of a vehicle water pump casting.



PhotoStress contoured shells ready for bonding to engine mount bracket casting.



Engine mount bracket with PhotoStress coating bonded in place. Coating covers entire surface except in the immediate area of the bolt holes, and other areas where fasteners and completion hardware would physically come in contact with the coating.





A plastic beverage bottle coated for comparison of PhotoStress and finite-element analysis.



An industrial food processing mixer coated around the vertical support and base.



Chair showing coating applied to areas of seat which was designed for greater flexibility.



PhotoStress coating applied to rapid transit vehicle wheel hub.



Newly designed universal joint coupling coated and ready for PhotoStress testing.





Filament-wound pressure vessel partially coated for testing. PhotoStress coating can be applied to any material regardless of its homogeneity.



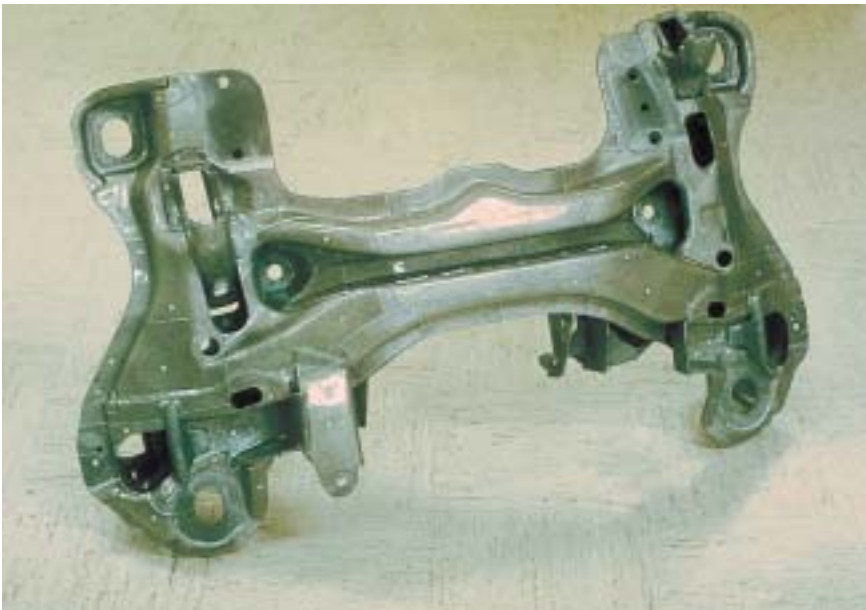
Typical samples that have been coated for conducting student experiments in PhotoStress testing at colleges and universities.



PhotoStress coating applied to a complex shaped augmentor fuel casting from a jet engine.



PhotoStress coating applied to an exploratory oil field drill head.



A complex-shaped automotive frame support member with PhotoStress coating applied.



A large pressure container with PhotoStress coating applied to a “ribbed” reinforced area.



Spherical pressure container with PhotoStress coating applied to entire surface area.



PhotoStress coating applied over the entire surface of a fan which was dynamically tested.



An automotive control arm bracket partially coated for PhotoStress analysis.



PhotoStress coating applied to track links from an earth-moving vehicle.



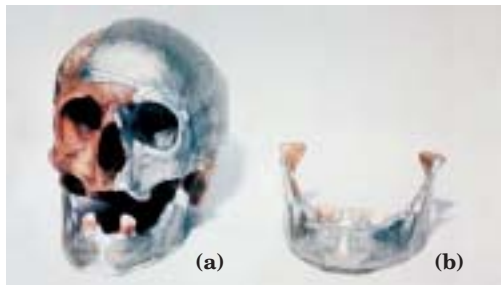
Coating ready for bonding to geared ring.



PhotoStress coating applied to the cast housing of a hydraulic drive system of a fire engine.



PhotoStress coating applied to a dental model used for design of bridge components.

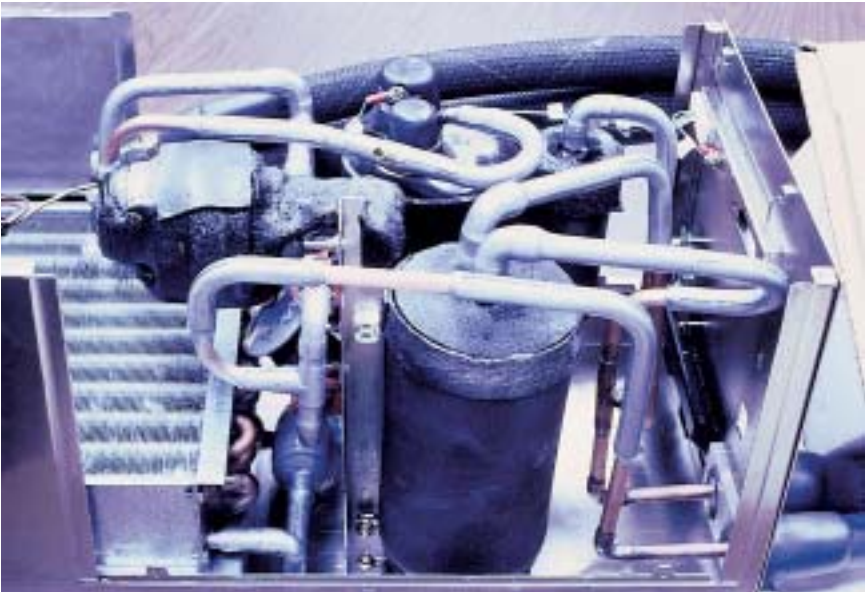


PhotoStress coating applied to human skull and jaw. (a) Subjected to shock loads representing blows from sharp and blunt objects. (b) Compressive forces were applied to simulate biting action.





A section of steam turbine blades coated for PhotoStress analysis under dynamic test conditions.



PhotoStress coating applied to tubing of a coolant system.

# Industrial Case History Applications

PhotoStress has an established history of successful applications in virtually every field of manufacture and construction where stress analysis is employed, including: automotive—farm machinery—aircraft and aerospace—building construction—engines—pressure vessels—shipbuilding—office equipment—bridges—appliances—plus many others. This section demonstrates the application of PhotoStress to a variety of stress analysis applications, including: assembly stress analysis, detection of yielding, residual stress analysis, anisotropic materials, dynamic stress analysis, and others.

## AIRCRAFT AND AEROSPACE APPLICATIONS

Many aircraft and aerospace parts and structures have been stress analyzed with PhotoStress coatings under both static and flight conditions. The method is very well suited for such applications since it provides full-field data on prototype structures.

*Airplane Window Frame.* Several tests have been performed on the window frame of a jet passenger transport. Figure 1 shows the color fringe pattern in the window frame when it was subjected to 98 percent of the maximum load. Note the stress concentration around the holes.



Fig. 1

*Wings and Access Doors.* The wings and fuel access doors of the Lockheed C-141 military jet transport have been analyzed under compression loads. The analysis of the stress distributions included both the elastic and elastoplastic ranges of deformation. In addition, one requirement was to establish the load that initiated elastic buckling. Buckling was observed during the loading of the wing while photographically recording the photoelastic pattern. The onset of buckling was evident by the sudden appearance of asymmetric high fringe orders on one section of the wing. The initiation of the buckling was detected photoelastically before any nonlinearities were observed in the displacement gages or the load record from the testing machine.

Figure 2 shows the PhotoStress pattern on a section of wing under 90,000 lb (20 KN) load. Note that the fuel access door, designed as a nonload-carrying member, exhibits higher stresses than the adjacent area of the wing. Figure 3 reveals the existence of permanent deformation in the reinforcing ribs of the fuel access door following removal of the load. In this view (the reverse side of the door) the residual fringes under no-load conditions testify to elastoplastic buckling of the ribs.



Fig. 2

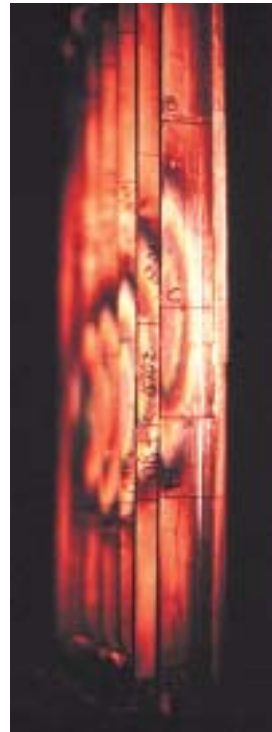


Fig. 3



*Landing Gears.* The landing gears for nearly all modern aircraft have been stress analyzed by covering the entire gear surface with PhotoStress coating. Landing gears are fabricated from forged and machined high-strength steel. The gear is a complex assembly of parts subjected to various static and shock loadings. Occasionally, certain parts are exposed to as many as six different loading conditions. Because the landing gear is used only twice during a flight and represents dead weight the remainder of the time, any weight reduction is of great benefit. At the same time, safety is obviously of paramount importance; large safety factors must be employed unless the stress distribution is accurately known for all significant modes of loading.

Figure 4 shows PhotoStress testing in progress on the main landing gear of the Airbus A330/A340 passenger aircraft. In this case, the



Fig. 4

*Photograph courtesy of Dowty Rotol Limited, Cheltenham, England.*

landing gear itself is a scale model made of an epoxy resin material for early design testing. After a thorough survey and analysis of the surface strain distribution on all structural components is completed, suggested changes are incorporated into the initial metal prototype. Additional Photostress analysis is then performed to help establish final design criteria prior to manufacture and acceptance testing of the actual landing gear.

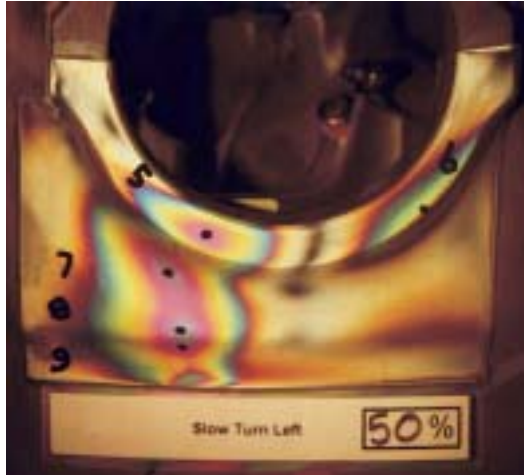


Fig. 5

Figure 5 shows a PhotoStress fringe pattern at a specific area of an Airbus gear during a static test sequence. Figure 6 below shows final prototype testing on a landing gear from a military jet fighter aircraft. In this case, the entire surface of the gear was coated for analysis. Figure 7 shows the PhotoStress fringe pattern over several sections of the landing gear.

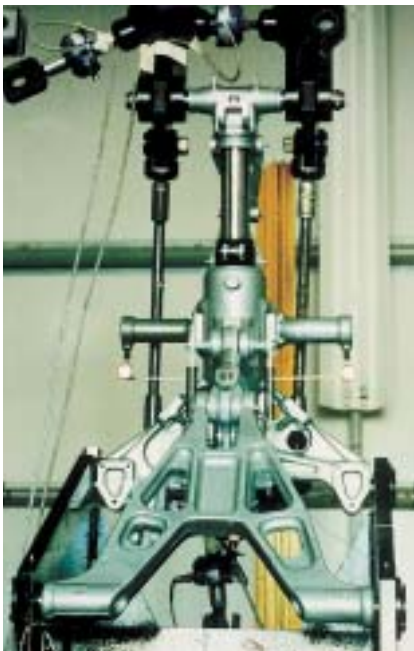


Fig. 6

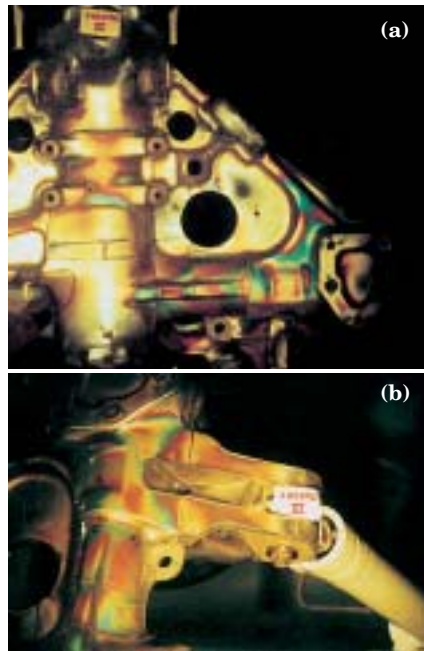


Fig. 7



Fig. 8

Figure 8 illustrates the PhotoStress fringe pattern on a partially coated prototype of the Boeing 767 main landing gear.

*Jet Engine Frames.* A section of a thin skin jet engine frame was PhotoStress coated to determine the location, distribution, and magnitude of the peak stresses in the vicinity of the struts and fuel pads. Simulated internal pressure was applied hydrostatically to the frame using a recirculating water system. Figure 9a shows the coated area of the frame, and Figure 9b illustrates the strain pattern observed at a specific location of the fuel pads and strut. It was clear that the maximum stresses developed between fuel pads. However, it was equally clear that the peak stresses were not present at the spaces where struts were positioned. Irregularities in the stress pattern at symmetrical points were attributed to minute dimensional changes during manufacturing such as mismatch at welds, local flat spots in curved skin, etc.

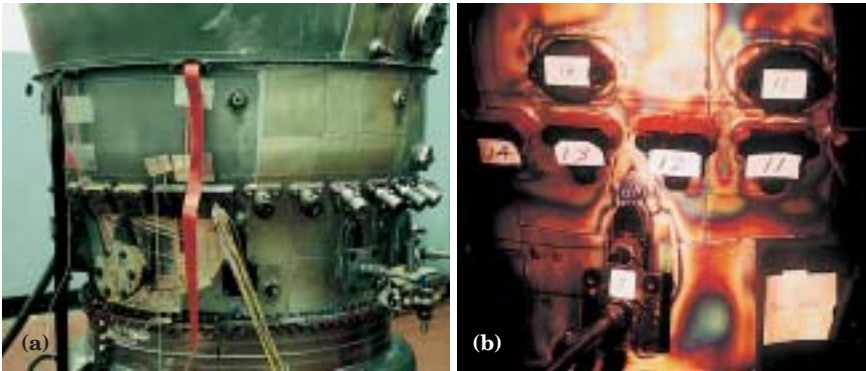


Fig. 9

*Jet-Engine Augmentor Control Casting.* Since the PhotoStress pattern reveals the overall strain distribution over the surface of a coated part, regions of low or zero stress areas are as important to recognize, as high-stress areas, since it may present an opportunity to remove material for weight savings. Removal of material in low-stress areas not only reduces weight, but helps in the redistribution and reduction of high-stress levels in adjacent regions. In the case of the augmentor control casting, a weight reduction test program was conducted to safely remove material to reduce weight. The surface of the casting was coated in its entirety and then pressurized. Low surface stress areas were identified, after which material was machined away from the inside of the casting in those areas. The augmentor casting was then retested and the change in stress distribution and magnitude analyzed. This process was repeated until an idealized stress/weight relationship was obtained. Figure 10a shows the augmentor casting coated and ready for testing, and Figure 10b shows the surface stress pattern during the pressurization sequence.

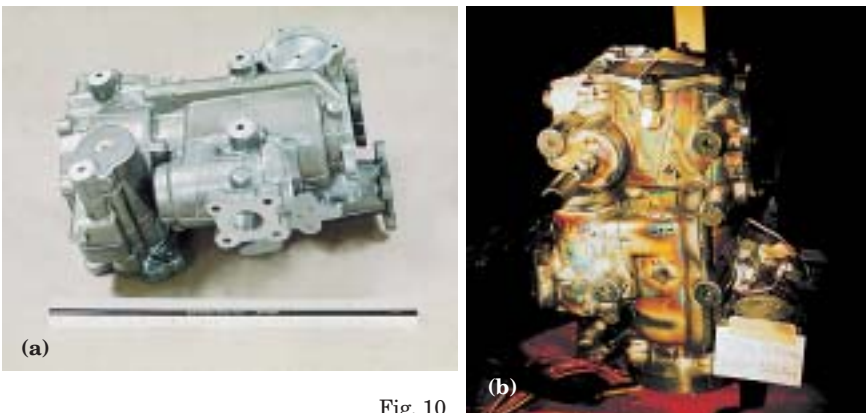


Fig. 10



*Aluminum Welded Joints on the Space Shuttle.* The response of PhotoStress coatings to inelastic deformation of the material to which they are bonded makes them extremely useful in analyzing aluminum welded joints. In general, an aluminum welded joint consists of a relatively weak, very ductile, small volume of filler material between two relatively strong, less ductile, large volumes of base material. As the joint is loaded, the stress state is three-dimensional, and the material deforms quite differently in the three orthogonal directions.

Joints of welded aluminum are very numerous in space structures, including the space shuttle, solid rocket boosters, fuel tanks, and the space station. Basic research included a PhotoStress analysis of the behavior of welded joints in the aft skirt of the solid rocket booster of the shuttle and in its new aluminum-lithium external fuel tank. In the aft-skirt study, joints were analyzed in uniaxial tension and pure bending. PhotoStress coating was bonded to welded specimens for both tensile and bending tests. The specimens were loaded in a computer-controlled, universal testing machine. Maximum shearing strains were measured during a load-hold-read sequence using a reflection polariscope equipped with an electronic uniform-field compensator, a telemicroscope, and a digital indicator/printer.

Figure 11 shows a typical tensile specimen, with its fringe pattern at 38 000 psi (260 MPa) tensile stress. Figure 12 shows a typical pure bending specimen with its fringe pattern at 17 000 in-lbs (1,920 N-m) moment. Welds in these specimens were 1.40-in (35.6-mm) thick (made in nine passes).

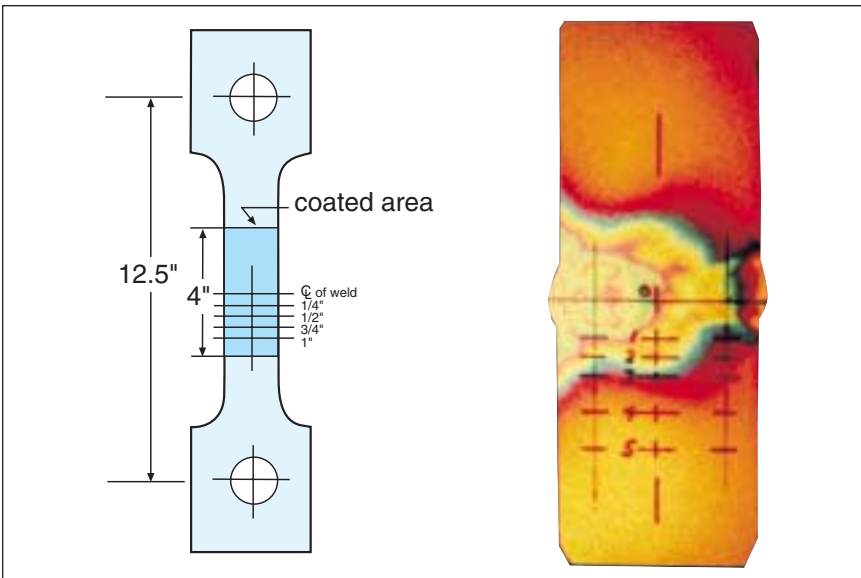


Fig. 11

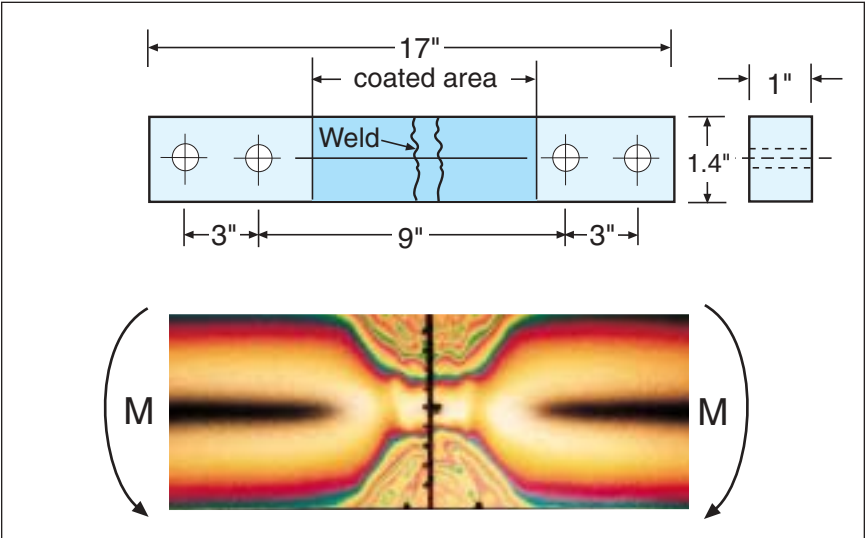


Fig. 12

Figure 13 shows a typical example of stress-strain curves obtained at various points in the aft-skirt tensile specimen. While they are not plotted in the figure, shearing strains greater than  $40\,000\ \mu\text{in/in}$  ( $40\,000\ \mu\text{m/m}$ ) were measured in the weld and heat-affected zone. Individual curves represent a fifth-order polynomial fit of data obtained from three repetitions of each test.

In the study of the external fuel tank, joints were analyzed in uniaxial tension. Figure 14 shows a typical fringe pattern at 32 000 psi (221 kPa) tensile stress. Note that fringes above and below the horizontal centerline of the weld (point 0) are different, indicating that one

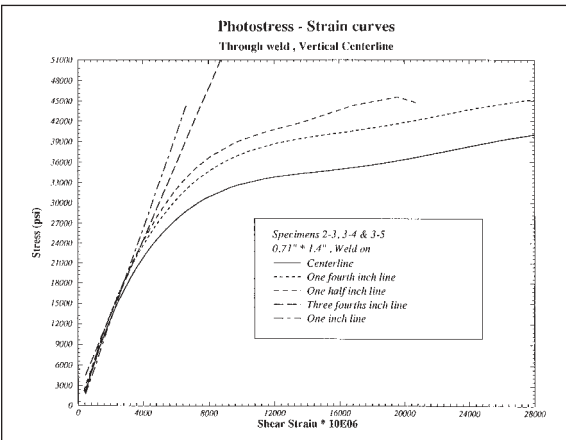


Fig. 13

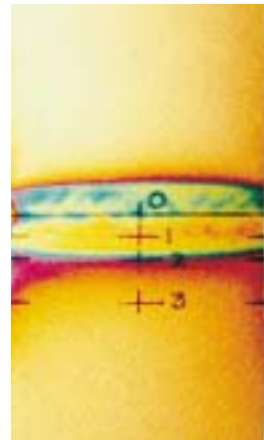


Fig. 14

fusion boundary [0.120 in (3.05 mm) above and below point 0] between the weld and base material is preferred for yielding (point 1). All specimens exhibited this behavior. Welds in these specimens were 0.20-in (5.08-mm) thick (made in two passes).

As part of the overall research effort, a full-scale test of a welded joint in the vicinity of a “hold-down” post on the shuttle aft skirt was conducted at the Marshall Space Flight Center in Huntsville, Alabama. A drawing of the location of the hold-down post on the skirt is shown in Figure 15, and the welded joint is identified in Figure 16. The fringe pattern observed in the photoelastic coating covering the welded joint when the test article was subjected to 70 percent of design limit load is shown in Figure 17. The test loads included tensile, torsion, and bending components applied simultaneously.

*This article was contributed by Dr. S.C. Gambrell, Jr. of the University of Alabama. Dr. Gambrell has done considerable research for NASA on strain analysis of welded joints as applied to the space shuttle.*

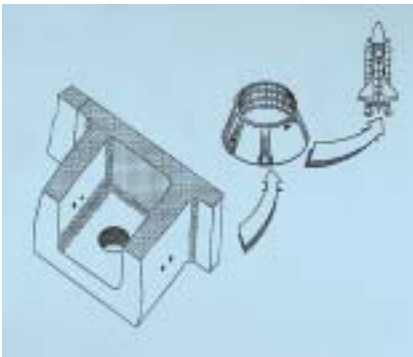


Fig. 15

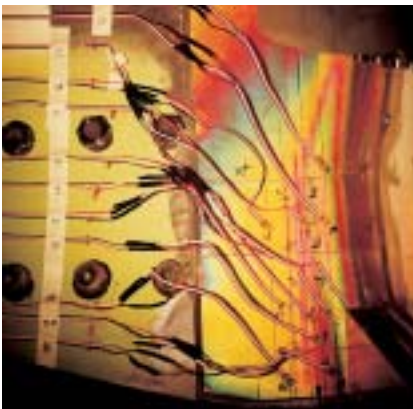


Fig. 17

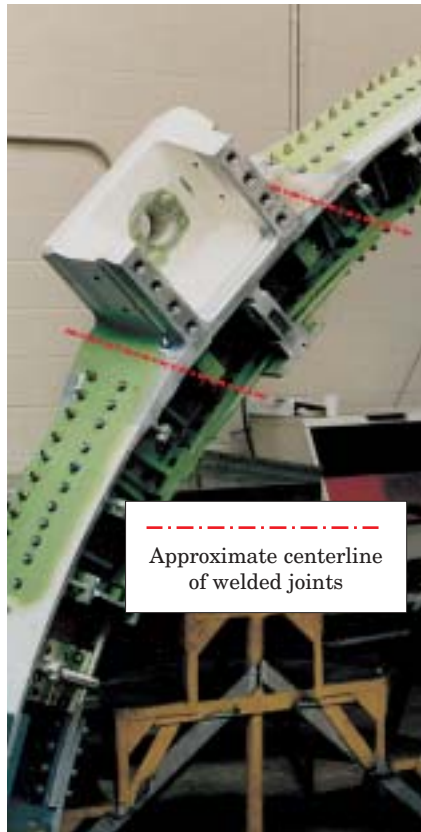


Fig. 16



## ASSEMBLY STRESSES

One of the most frequently ignored situations that can produce unexpected high stresses occurs during the assembly of components which make up the whole of the part or structure. It is not unusual for local yielding to occur when bolts are tightened, or when parts are pressed into place; and, although such yielding may not necessarily impair the safety of the structure, experience has proven in countless instances that fatigue cracks often develop in regions where alternating service stresses are superimposed upon high-assembly stresses. If they exist, assembly stresses become immediately apparent when a PhotoStress coating is applied to the part prior to assembly.

*Aluminum Support Post.* PhotoStress testing determined the primary cause of structural failure at the base of an aluminum post used to support traffic lights, signs, etc. Figure 18 shows the coated post, and Figure 19 shows that yielding occurred in the welded area of the base after the bolts were tightened. Adding service loads to the pre-existing high-tensile stress condition caused the premature failure. PhotoStress analysis also suggested that the detrimental effects of assembly could be greatly reduced by modifying the cast base. This was accomplished by introducing a slight degree of concavity into the bottom surface of the base, which placed the initial assembly stresses in compression instead of tension. With this modification, future failures were eliminated.



Fig. 18



Fig. 19

*Diesel Engine Flywheel.* A diesel engine flywheel was failing around the bolt circle. Figure 20 shows an unmounted flywheel coated with PhotoStress plastic, and then bolted to the diesel engine for dynamic testing. When the bolts were tightened, very high stresses appeared, which were well above the design limit of the material as shown in Fig. 21a. Superposition of forces due to dynamic testing caused premature fatigue failure. The major problem was thus defined by PhotoStress analysis as one of assembly-induced stresses. Redesign of the flywheel (where it mated to the shaft of the diesel engine) significantly reduced the initial assembly stresses as shown in Fig. 21b.

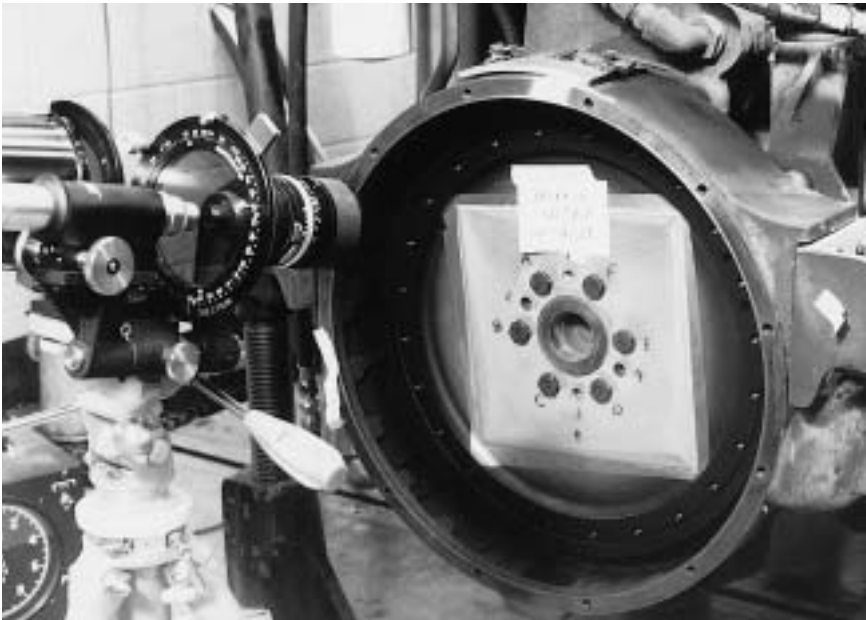


Fig. 20

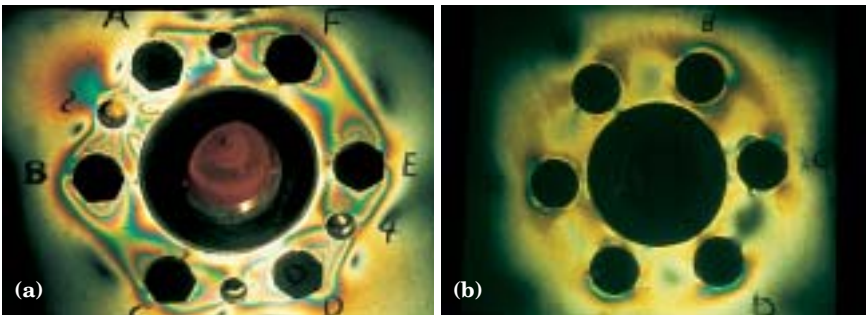


Fig. 21

*Suspension Mounting Bracket.* A suspension mounting bracket was bolted to its mating part on a truck frame. The bracket was first coated, and then bolted in place at a specified torque level. After bolting, a PhotoStress fringe pattern appeared in the coating, which revealed stresses due to the assembly process as shown in Fig. 22a. Test forces were then applied to the bracket and Fig. 22b shows the new stress pattern due to the combined assembly/external load conditions.

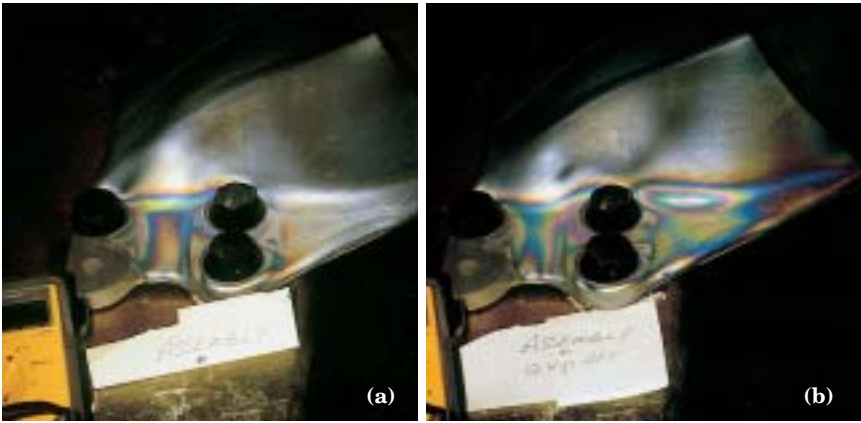


Fig. 22

### APPLICATIONS TO COMPOSITE (HETEROGENEOUS) MATERIALS

PhotoStress coatings can be applied to almost any material; this includes applications to composite materials such as reinforced plastics, concrete, wood, and metal-matrix composites. Due to their inhomogeneity, most composite materials have mechanical properties that vary from point-to-point. Very commonly, such materials are also anisotropic in their mechanical properties, and the magnitudes of the properties (elastic modulus, Poisson's ratio, ultimate strength, etc.) at each point vary with the direction at the point. As a result, the stress and strain distributions in composite members are apt to be far from intuitively obvious, and localized strain measurements (as with strain gages, for instance) may be seriously misleading.

Because of its full-field capability, PhotoStress is ideally suited for preliminary stress analysis of test objects made from composite materials. It reveals the detailed strain distribution and the principal strain directions over the entire coated surface of the part. As exemplified by some of the illustrations in this article, the coating also tends to display the underlying structure of the inhomogeneities.

*Effect of Fiber Reinforcement on Strain Distribution.* A fiberglass plate and an aluminum plate of similar dimension were coated with PhotoStress plastic and tested in uniaxial tension. The resulting strain patterns that developed around the holes in both plates were similar in geometry, demonstrating a definite correspondence in the gross strain distribution in homogeneous and heterogeneous materials. However, the fringe patterns appeared as smooth unbroken lines for the homogeneous material (aluminum) as shown in Fig. 23, while for the heterogeneous material (fiberglass), they were discontinuous, with a more-or-less scotch plaid appearance as shown in Fig. 24. In another example, Figure 25 shows the strain pattern on a simply loaded fiberglass/honeycomb beam.

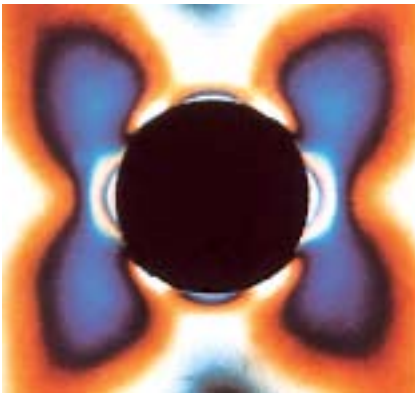


Fig. 23



Fig. 24

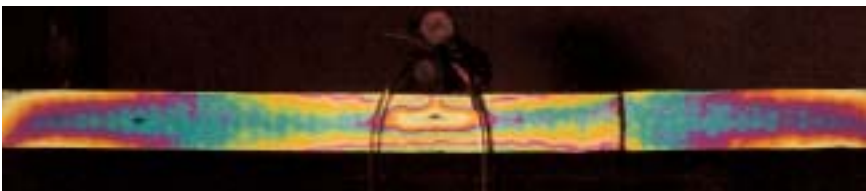


Fig. 25

*Filament-Wound Pressure Vessel.* PhotoStress testing of a filament-wound pressure vessel was undertaken because of unexpected and unusual results of measurements made with strain gages. In use, the composite material pressure vessel was packed with solid propellant and used in an aerospace application, as shown in Fig. 26. After the filament winding was completed, a circular section was cut out for mounting a nozzle, and strain gage measurements were to be made at

symmetrical points tangent to the cut-out edge. After the gages were installed and the vessel pressurized, the strain measured was grossly inconsistent from one symmetrical point to the other. It was then decided to apply a PhotoStress coating to a test vessel (Fig. 27) to get a clear picture of the strain distribution around the cut-out to help explain the erratic strain gage results. The fringe pattern (Fig. 28) clearly shows the reason for the differing strain gage results around the edge of the cut-out. Instead of the assumed uniform strain distribution around the cut-out, a repeatable series of alternating fringes, with low strain areas in between, accounted for the erratic strain gage readings. Some gages were placed over the higher strain fringe areas, while others were placed between fringes. The reason for this unforeseen strain distribution lies within the geometry of the filament-winding process. At the conclusion of the winding, the final layer of glass

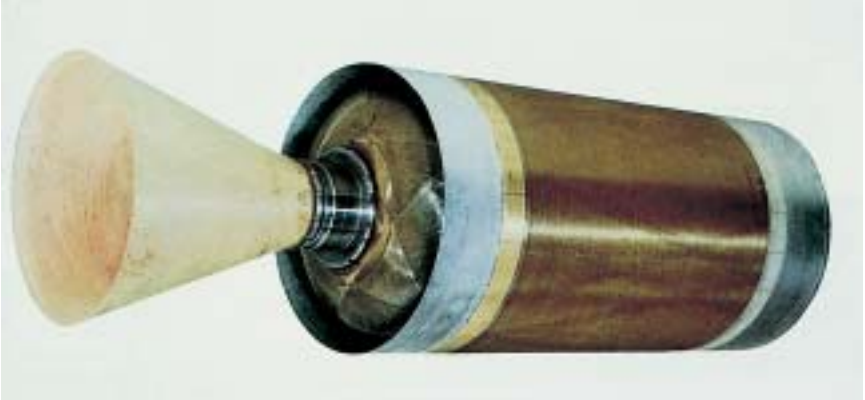


Fig. 26



Fig. 27

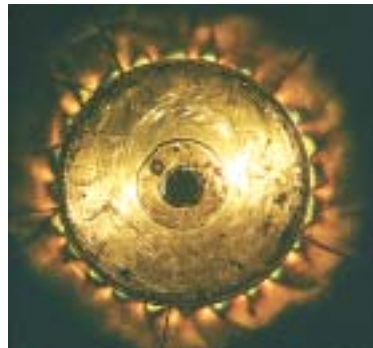


Fig. 28



rovings before and after the cut-out is depicted in Fig. 29a and b. Thus, when the vessel was pressurized, there was less surface strain at the boundary cut-out where the last roving was laid, and higher strain between rovings.

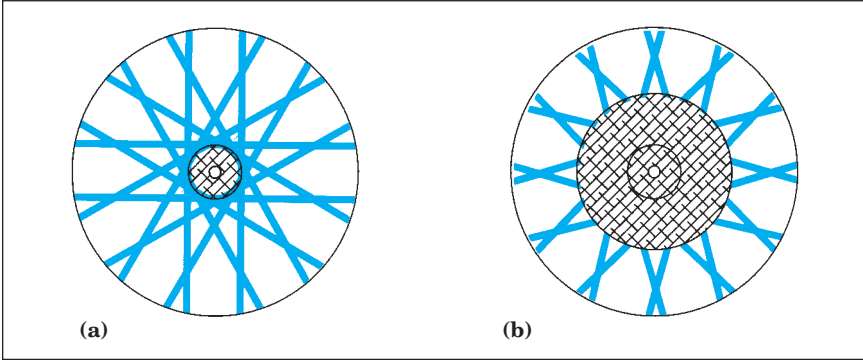


Fig. 29

*Wood, Rock Salt, and Honeycomb Applications.* Figure 30 shows a PhotoStress fringe pattern over the cross section of a wooden beam. This study was in support of analyzing shrinkage stresses during drying. Figure 31 is an analysis of a composite honeycomb panel subjected to a tensile load. A crack was introduced into the panel and the strain distribution analyzed during crack propagation. Figure 32 shows the strain distribution on a core of rock salt under a compressive load. This test was conducted to assist in the structural analysis of tunneling in a salt mine.



Fig. 30

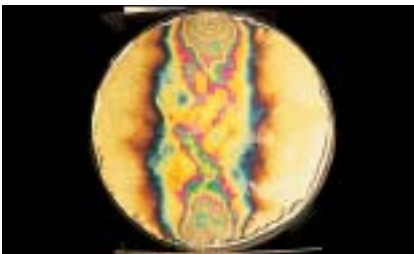


Fig. 32

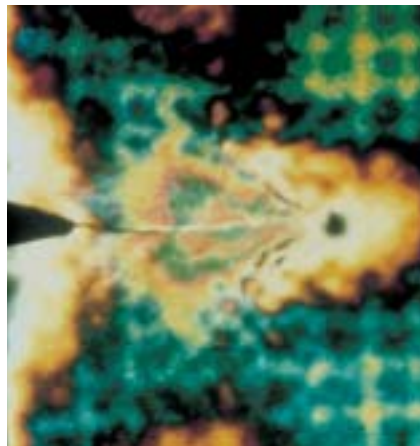


Fig. 31

*Strain Distribution in Concrete.* PhotoStress coating was applied to one face of a concrete block, and the block was loaded in compression. Since concrete is a heterogeneous mixture of high-modulus aggregate (stone) and low-modulus cement, the strain is distributed nonuniformly between the stones and cement, with the highest strains occurring in the cement as shown in Fig. 33. Measurements revealed that local strains were as high as four times the average strain as shown in Fig. 34. To analyze the strain distribution in the aggregate only, a photoelastic model was made in which the cement was masked out. The resulting fringe pattern shown in Fig. 35 demonstrated that the relative position of the stones influenced the load flow.



Fig. 33

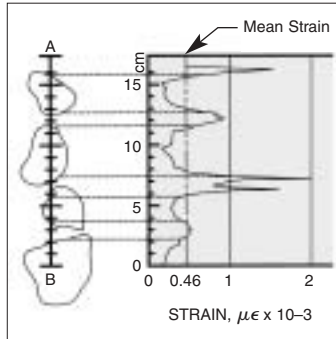


Fig. 34

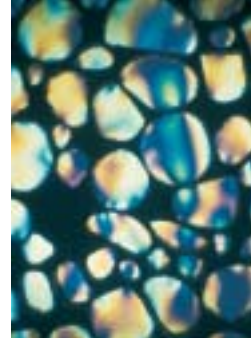


Fig. 35

## RESIDUAL STRESSES

The detection and measurements of residual or “locked-in” stresses in a part has long been an important, and often elusive, problem for the design engineer. Residual stresses are usually introduced in a material during manufacturing processes, such as casting, welding, machining, molding, heat treatment, etc. Residual stresses, as defined here, should not be confused with stresses caused by the assembly of component parts. The separate subject of assembly stresses is treated on page 22.

The effects of residual stress may be either beneficial or detrimental, depending on the distribution, magnitude, and sign of the stress with respect to the load-induced stresses. In many cases, residual stress is detrimental, and is the predominant factor contributing to the structural failure. There are several practical methods used to detect and measure residual stress, each having advantages and disadvantages. With PhotoStress, the principal advantage is that the presence of residual stress is revealed everywhere it occurs on the surface of a part. The disadvantage is that the part must be cut or sec-



tioned to reveal any residual stress present. In the following examples, PhotoStress was used to solve design problems where residual stress was found to be the principal cause of failure.

*Metal Fan Hub.* A metal fan hub was failing in service where the hub shaft support was welded to the flange. Analytical studies predicted low stress levels during the dynamic loading sequence. Strain gage measurements near the weldment supported this prediction.

Several of the fan hubs were fabricated for test purposes, and PhotoStress coatings were contoured and bonded over the surface area. After application of the coating, the hubs were sawed through, releasing the internal forces (residual stresses) developed by nonuniform heating during the welding process. The fringe patterns in the PhotoStress coating shown in Fig. 36a revealed locked-in residual stresses, which were of very high magnitude in the welded area. The modest cyclic stresses, superimposed upon the high residual mean stresses, were sufficient to produce field failures.

Subsequent test samples were stress-relieved after fabrication, and PhotoStress analysis of the stress-relieved hub showed no evidence of residual stress after cutting, as shown in Fig. 36b.

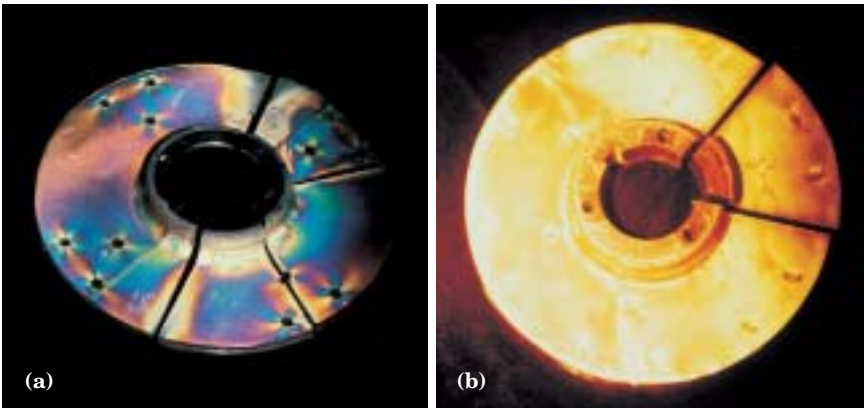


Fig. 36

*Washroom Sink.* A new plastic material was developed for washroom sinks. The sinks were fabricated by a hot-mold process, and several sinks were installed. Within a relatively short time, cracks began to appear around the drain area. To determine the cause of failure, a PhotoStress coating was applied to the inside and outside surfaces in the drain area as shown in Fig. 37a. The following tests were conducted: (1) assembly stress analysis when the metal drain was installed; (2) thermal stress analysis due to hot and cold water cycling; and (3) residual stress analysis.

PhotoStress analysis showed that drain installation produced no significant assembly stress pattern, and the hot and cold water cycle test produced only a small effect. The most significant results appeared when the residual stress test was conducted. This was accomplished by cutting through the sink and the attached PhotoStress coating in several areas. When a cut was made through the drain area, the PhotoStress pattern revealed a significant locked-in stress as shown in Fig. 37b. The major cause of failure was thus determined to be the residual stresses built into the sinks during manufacture. The sinks were later annealed after initial hot-mold fabrication, eliminating the residual stress problem and ultimate failure.

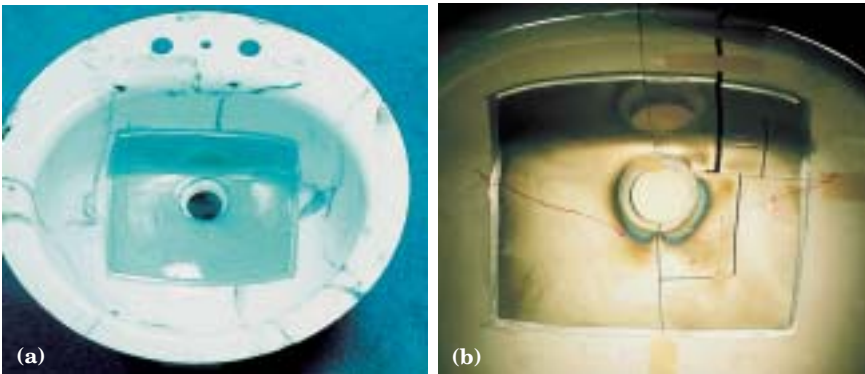


Fig. 37

*Diesel Engine Cylinder Head.* Among the many applications where PhotoStress testing is used at Consolidated Diesel Corporation\* (CDC), the recognition and measurements of Residual Stress is regularly applied. Anytime a vendor experiences a change in the manufacturing process of a supplied part, the Cummins Engineering Standard (CES) determines the requalification of that part before it is released to production. For many common castings, such as blocks and heads, this equates to a determination of the residual stress—both acceptable limits and comparative changes from previously accepted processes.

Triggers for this testing might be a supplier, or changes to changes in the heat treatment, changes in the in-mold cooling rates, changes in the casting's direction of pouring, or significant changes in mass for a redesigned part.

\*Consolidated Diesel Corporation is a joint venture between Case New Holland (CNH, formerly Case) and Cummins, Inc. (no longer Cummins Engineer Company, nor CECO), manufacturing mid-range diesel engines (60 to 350 hp). Cummins also manufactures heavy duty (300 to 525 hp) and high horsepower (450 to 6,000 hp) engines.



Fig. 38



Fig. 39

One such example of the detection and measurement of residual stress after a process change in a cylinder head casting is illustrated in the above figures. Figure 38 shows the cylinder head after PhotoStress coating has been applied, and Fig. 39 shows the reflection polariscope set-up for the measurement process. Figure 40 shows the cylinder head after sectioning, and Figure 41 shows the residual stresses relieved at one particular section of the head.



Fig. 40



Fig. 41

### DETECTION OF YIELDING

A PhotoStress coating will permanently record any plastic strain which occurs in the test part after the coating has been applied. Thus, PhotoStress is an extremely useful tool for detection of yielding. Observation of the coated part after the removal of external loads will highlight any regions where local yielding has occurred. Analytical methods cannot infallibly predict the occurrence of localized yielding since it is random and its exact location is unpredictable. Electrical resistance strain gages are not reliable indicators for localized yield detection, since they are point-measuring devices, and may or may not be installed in the specific area where the onset of plastic deformation occurs. Recognition of yielding using PhotoStress, however, is easily accomplished. When a coated part or structure is observed under load,

the colorful stress pattern appears. After the load is removed, the color pattern will disappear in all areas that return to their original state. In areas where deformation remains as a result of yielding, a color pattern will also remain. PhotoStress is even capable of detecting the onset of initial yielding in the form of slip bands, or Lueder's lines, which is especially important in material research and proof testing. Described below are a few examples of yield detection using PhotoStress.

*Aircraft Ejection Seat.* PhotoStress coatings were bonded to parts of a military aircraft ejection seat. The seat, containing a dummy pilot, was installed in a fuselage section for testing. Once ejected, the seat and dummy were returned to earth by parachute as shown in Fig. 42. The PhotoStress-coated sections of the seat were then observed with a reflection polariscope to detect yielding that occurred during the test event as shown in Fig. 43.



Fig. 42

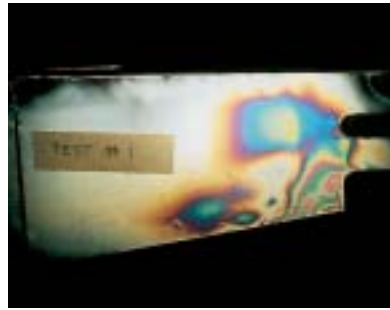


Fig.43

*Materials Testing.* PhotoStress was used to study the post-yield strain behavior on “notched” tensile test specimens. Figure 44a shows a broad plastic strain field developing over most of the surface of one test sample, while Fig. 44b shows initial yielding occurring in the form of Lueder's lines (slip planes) in the other.



Fig. 44

*Pressure Vessel.* A PhotoStress-coated pressure vessel was subjected to combined axial compression loads and internal pressure as shown in Fig. 45a. At proof pressure, a severe stress concentration, which resulted in yielding, was observed in a joint area of the pressure vessel illustrated in Fig. 45b.

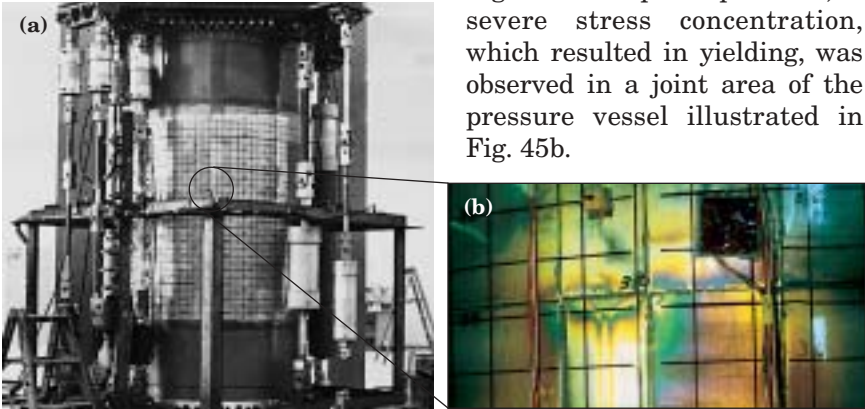


Fig. 45

*Lueder's Lines.* A different technique can be employed where yielding is to be detected inside a pressure vessel. The procedure is as follows:

1. Coat the inside of the vessel in the area of interest.
2. Pressurize the vessel to a predetermined level; after emptying it, examine the coating for any permanent fringe patterns.
3. If no pattern is observed in Step 2, repeat this procedure at higher pressure levels until permanent patterns are observed or the maximum allowable pressure is reached.

Figure 46 shows such a permanent fringe pattern in the form of Lueder's lines, observed on the interior wall of a large, thick walled pressure vessel after proof testing.

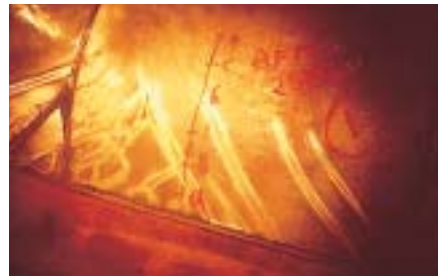


Fig. 46

## PHOTOSTRESS IN THE BIOMECHANICS FIELD

Among the more intriguing and significant applications for PhotoStress testing are those in the field of biomechanics. Areas of application, to name a few, include stress analysis of skeletal parts such as the femur, pelvis, and skull; knee, elbow, and other joint replacements; dental implants and bridges; and mechanical medical aids such as forceps and surgical staplers.



*Hip Replacements.* Particularly noteworthy is the extent to which PhotoStress is being used in the analysis of stresses for total hip replacement. This work is being conducted both at orthopedic research clinics and by manufacturers of prosthetic devices. According to one medical research group, the use of PhotoStress on bone has a distinct advantage over other strain-measurement methods such as finite-element analysis, brittle coatings, strain gages, and photoelastic modeling. Each of these methods has limitations in its application to the study of bone, including directional and positional constraints, and assumptions of homogeneity. Because of its full-field capability, PhotoStress overcomes these limitations by permitting observation and measurement of strain directions and magnitudes, under varying complex load modes, regardless of material homogeneity. A few examples of the application of PhotoStress to bone are shown here.

*Example 1.* PhotoStress analysis of the proximal femur was undertaken to evaluate the stress transfer for total hip replacement. Figure 47a shows the fringe pattern on the femur before the implant was inserted. Figure 47b shows the implant in place, and Fig. 47c and 47d show the change in strain distribution on the surface of the femur when compared to the photo before implant.

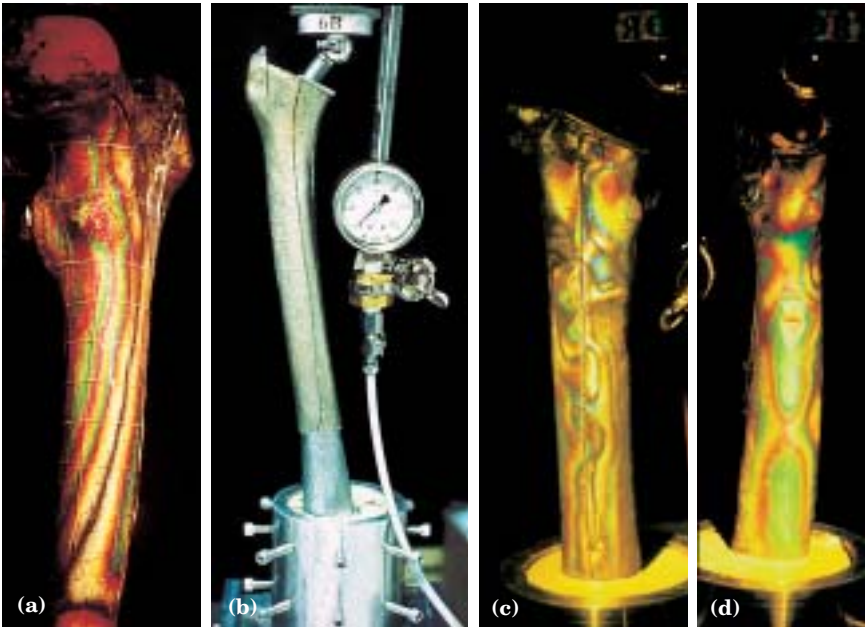


Fig. 47



Example 2. Figure 48a shows simulated femoral test specimens being prepared for PhotoStress analysis of various types of hip implants, and Fig. 48b shows the resulting stress distribution of the different implants used. After the modeling tests have been completed, selected prosthesis are then chosen for implant in real bone for further PhotoStress testing.



Fig. 48

### ANALYSIS OF RUBBER AND OTHER ELASTOMERIC MATERIALS

The past several decades have seen elastomers progress into their present role as powerful and versatile engineering materials. Many industrial applications are nonstructural and require little or no quantitative technical analysis. In other instances, predictable and repeatable structural response is necessary, requiring sophisticated and quantitative understanding. Elastomeric deformations in the 50 to 100 percent strain range are not uncommon. These high strains and

large deflections, combined with nonlinear viscoelastic mechanical properties, serve only to make theoretical analysis of complex-shaped, three-dimensional elastomeric parts very uncertain. Experimental verification is highly desirable in such instances.

Obtaining valid stress/strain measurements on elastomeric components is also unique in that most conventional transducers, including electrical resistance strain gages, produce unacceptable mechanical reinforcement. Consequently, the value of the uncorrected “as-measured” strains can be several orders of magnitude less than the actual strain in the elastomer when there is no strain gage installed. Therefore, more compliant sensors, which produce less mechanical reinforcement, are clearly more desirable for use on elastomeric materials. Of course, whenever possible a noncontacting measurement scheme is preferred. For example, it becomes practical to use a conventional measurement scale to directly measure the deformation between two points on elastomeric tension samples (providing that the elongation is sufficiently large).

In the more usual case of irregularly shaped elastomeric product designs, highly localized strain/stress gradients and concentrations may be present; and choosing an acceptable experimental measurement technique becomes increasingly difficult. In these situations, one of the preferred strain measurement methods is the PhotoStress technique, using low-modulus coatings to minimize the undesirable mechanical reinforcement. The figures in this section show some typical cases where PhotoStress has been used successfully on low-modulus or elastomeric materials.

*Automobile Tire.* Tests were conducted to better understand the stress behavior of automobile tires. Tires were coated with photoelastic plastic on the outside rubber surface and directly on the reinforcing cords after rubber removal. Because the strains were very high, thin low-modulus coat-

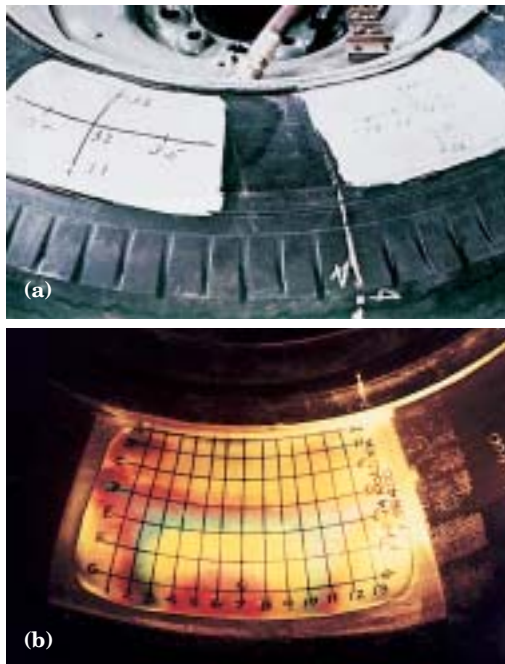


Fig. 49

ings—usually 0.040 in. (1 mm) thick or less—were used for this application. Analysis was made for tires subjected to the following loading conditions: (1) internal pressure, (2) pressure plus an external vertical load, and (3) pressure plus an external load plus rotation of the tire. Figure 49a shows the coating applied to the sidewall area. Figure 49b shows the PhotoStress strain pattern when the tire was subjected to a vertical load.

*Oil Well Casing Packers.* High elongation PhotoStress coatings were applied to steel-wire-reinforced low-modulus packers used in oil wells. The structural response to internal pressure and casing confinement was not completely understood, and the PhotoStress method was used to gain a better quantitative understanding of the strain distribution on the packers. Figure 50a shows a typical packer with the high elongation coating installed and ready for pressure testing. Figure 50b shows the strain pattern at a particular internal pressure level applied to the packer. Ongoing tests were performed after installing the packers inside the metal casings, and observing the strain pattern at the packer ends resulting from length changes caused by the restraint of the casing.

*Solid Propellant Grain.* Figure 51 shows a pattern of thermal stresses observed on solid propellant grain (low-modulus material). The strain pattern developed due to constraints imposed by the rocket casing during cooling of the propellant to room temperature after casting.

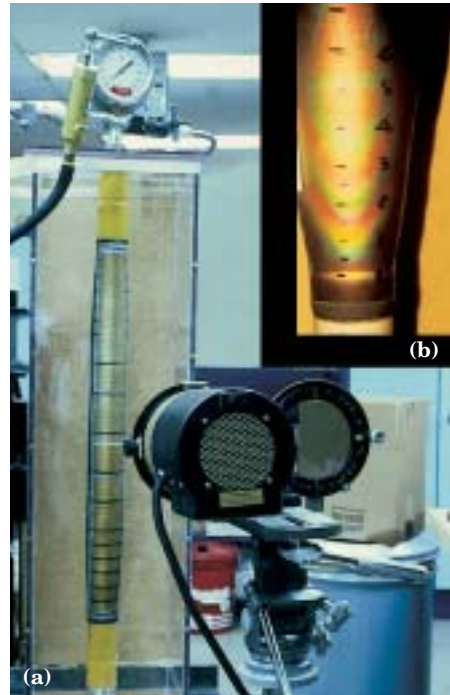


Fig. 50

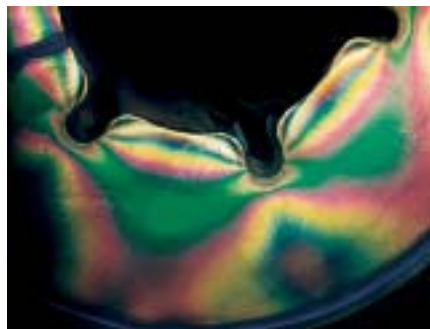


Fig. 51

## DYNAMIC TESTING

For dynamic stress analysis involving cyclically varying strains of fixed magnitude and frequency, the standard reflection polariscope light source is replaced by a stroboscopic light in order to make the fringe pattern appear stationary. The procedure for performing dynamic strain measurements under stroboscopic lighting are the same as those for static strain measurement. PhotoStress testing can also be used to observe stresses due to impact, such as those caused by shocks, explosions, and other high-speed events. In these cases, the fringe patterns can be captured using high-intensity light sources in conjunction with the reflection polariscope, and high-speed cameras. The newly developed PhotoStress Plus system incorporates a digital video camera that permits dynamic Photostress testing up to 30 Hz.

*Industrial Fan.* A photoelastic coating was applied to the hub and blades of an axial-flow fan. The fan was dynamically balanced and then operated at normal rotational speed. Two tests were conducted to assess the merits of two different blade retainers. A reflection polariscope fitted with a stroboscopic light was used for the measurements, and synchronization of the stroboscope and fan was accomplished with a photoelectric cell. The discontinuous light intensity needed for the photocell signal was obtained from a piece of black tape on one area of the fan shaft. The following conditions were found:

1. Assembly stresses greatly exceeded dynamic stresses and produced plastic deformations in certain areas.
2. Centrifugal stresses were negligible.
3. Stress concentrations were almost totally absent in the blade fillet area, indicating excellent force transmission between the blade and hub during fan rotation.
4. One of the blade retainers created assembly stresses three times higher than the others.

The coated fan is illustrated in Fig. 52 and the dynamic test setup is



Fig. 52



Fig. 53



Fig. 54



Fig. 55

shown in Fig. 53. Figure 54 shows the static strain pattern produced by assembling the hub to the shaft, and Fig. 55 shows the assembly strain pattern in the fillet of one blade.

*Dryer Fan.* In another case, PhotoStress was used to analyze the stress distribution in a newly designed fan for a household clothes dryer. Figure 56 illustrates the fringe pattern revealed during rotation of the fan at a specified test speed.

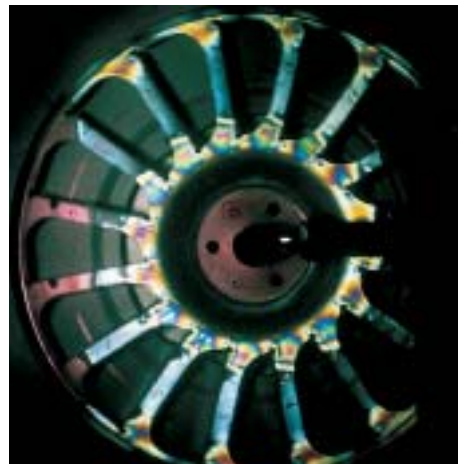


Fig. 56



*Diesel Engine Castings.* Jacobs® Vehicle Equipment Company, a division of Danaher Corporation, designs and manufactures a line of well known Jake-Brake® compression release engine retarders. These are hydraulic devices which transform conventional diesel engines into energy absorbers rather than energy sources. In practice, these brakes serve to retard the vehicles (trucks and buses) on flat roads or to control their speed as they descend steep grades.

Complex cast-metal housings, containing multiple internal hydraulic circuits, are mounted over the rocker arms of the diesel engine. When the hydraulic circuits are activated, the Jake Brake modifies the open/close cycles of the exhaust valves of the engine. Understanding the dynamic stress fields produced by the cyclical pressure in the internal hydraulic circuits is a challenging analytical assignment. Further, it is equally difficult to predict the locations and magnitudes of the localized assembly stresses produced by bolting the brake housings to the engine. And, finally, fatigue considerations require that the cyclical stresses be accurately superimposed on these steady-state assembly stresses. Jacobs Vehicle has used the PhotoStress method to better their understanding of these operational stress fields.

Figure 57 shows two typical housings with the PhotoStress coatings bonded in place. Each test housing is bolted to its own unique fixture which simulates the actual mounting pads common to the diesel engine. This housing/fixture assembly is used in conjunction with a conventional hydraulic testing machine to apply:

---

*Jacobs® and Jake Brake® are registered trademarks of the Jacobs Vehicle Equipment Company.*



Fig. 57

- cyclical pressure to the internal hydraulic circuits
- cyclical external loads simulating the reactions against the diesel exhaust valves, etc.

The test sequence begins by first bolting the housing to the test fixture, and then observing the PhotoStress coating with a reflection polariscope to locate and measure points of initial assembly stress. Following static analysis of the assembly stresses, a stroboscopic light is installed on the reflection polariscope for observation and measurement of the stresses when the dynamic loads are applied. Figure 58 shows a typical test setup. The insert shows the PhotoStress fringe order on a typical Jake Brake housing resulting from bolting (assembly) only. These are the mean or static stresses. The combined fringe orders pattern when the superimposed internal hydraulic pressure load is applied is then obtained. The difference between these two loading conditions establishes the cyclical, or alternating, stress level.

When observing the dynamic event, a slow-motion feature built into the stroboscopic control unit is engaged. This reveals the cyclical pressure-induced stress field which is superimposed on the pre-existing steady-state assembly stress field. This static/dynamic test sequence is very valuable in first identifying and then quantifying stresses in areas where fatigue is a design consideration.

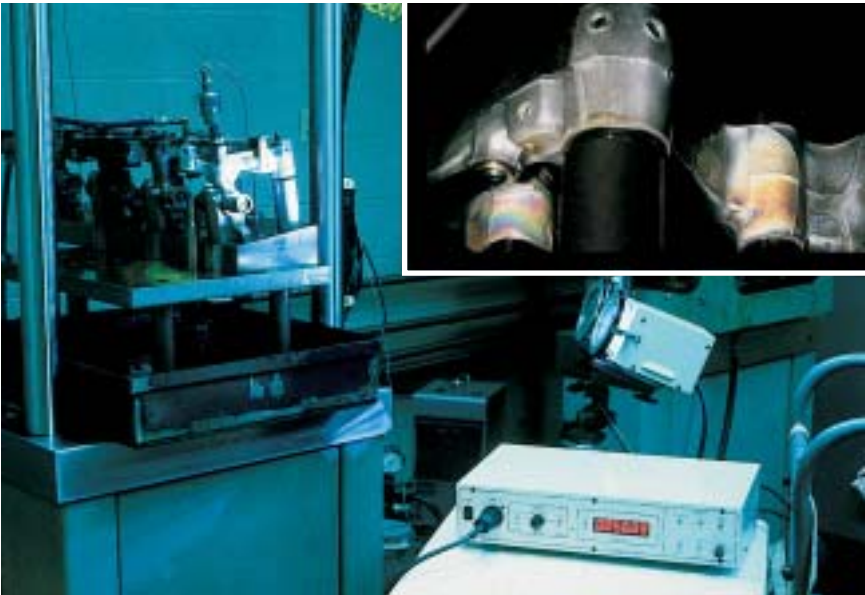


Fig. 58

## PHOTOSTRESS AND FINITE-ELEMENT ANALYSIS

When finite-element analysis (FEA) first established itself as a fast and convenient approach to structural design analysis, it was envisioned by many people as a replacement for conventional strain/stress measuring techniques such as strain gages and photoelastic methods. With today's sophisticated computer software programs, FEA is now widely used to help solve complex stress problems, and to refine the geometry of a design prior to building the part or structure. But the design process for maximizing structural integrity and putting the product into service almost always requires qualification testing to verify the computed results.

In regions of stress concentration, for instance, the accuracy of FEA is significantly affected by the type of element selected and the nodal spacing. A few quickly and inexpensively made photoelastic measurements can be used to test the accuracy of the numerical results and serve as a guide for refining the finite-element model. With more sophisticated hybrid techniques, the photoelastic measurements are entered directly into the computer program, commonly as nodal values at free boundaries. This type of procedure is particularly effective since it uses one of the strengths of photoelasticity to compensate for potential frailty of numerical methods; namely, the reliably accurate determination of boundary stresses.

The following procedure describes a simplified application in which PhotoStress complements FEA for achieving optimal and verifiable stress analysis of a design.

- Perform PhotoStress testing on a scale model of the part. The model materials and size are selected to permit developing readily measured fringe orders with conveniently small loads.
- Conduct an FEA analysis of the model to yield the difference in principal strains ( $\epsilon_1 - \epsilon_2$ ) at the nodal points. This information is displayed graphically in colors to correspond to the colored fringe pattern obtained with PhotoStress.
- Compare the colored patterns from PhotoStress and the numerical calculations. On the basis of agreement or disagreement between the patterns, modify the FEA model as necessary to yield the correct stress distribution corresponding to the PhotoStress pattern. When the two patterns are in full agreement, the individual principal strains can be obtained by FEA, avoiding the necessity for photoelastic separation of the principal strains.
- Fabricate the full-size real part on the basis of the final FEA model. Follow-up PhotoStress and/or strain gage measurements can then be made at selected points on the part to validate the computed results.

The foregoing procedure was used in the stress analysis of a 160t crane hook, fabricated from steel plate. A 1/10 scale plastic model of the 3.5 m hook was made, and coated with PhotoStress plastic. With a 1000N load on the model, the isochromatic fringe pattern (strain magnitude) is shown in Fig. 59a, and the black isoclinic pattern (strain direction) in Fig. 59b. For numerical analysis, the FEA mesh is illustrated in Fig. 59c, while Fig. 59d and 59e show the computer-generated isochromatic and isoclinic fringe patterns. Comparison of Fig. 59a and 59b with Fig. 59d and 59e demonstrates very good agreement between the experimental and numerical results. The  $\sigma_x$  principal stress profile was then computed as shown in Fig. 59f.

*This article was contributed by B. Mynar, P. Sperka, M. Vasicek, Department of Construction and Transportation Machines, Technical University of Brno, Brno, Czech Republic.*

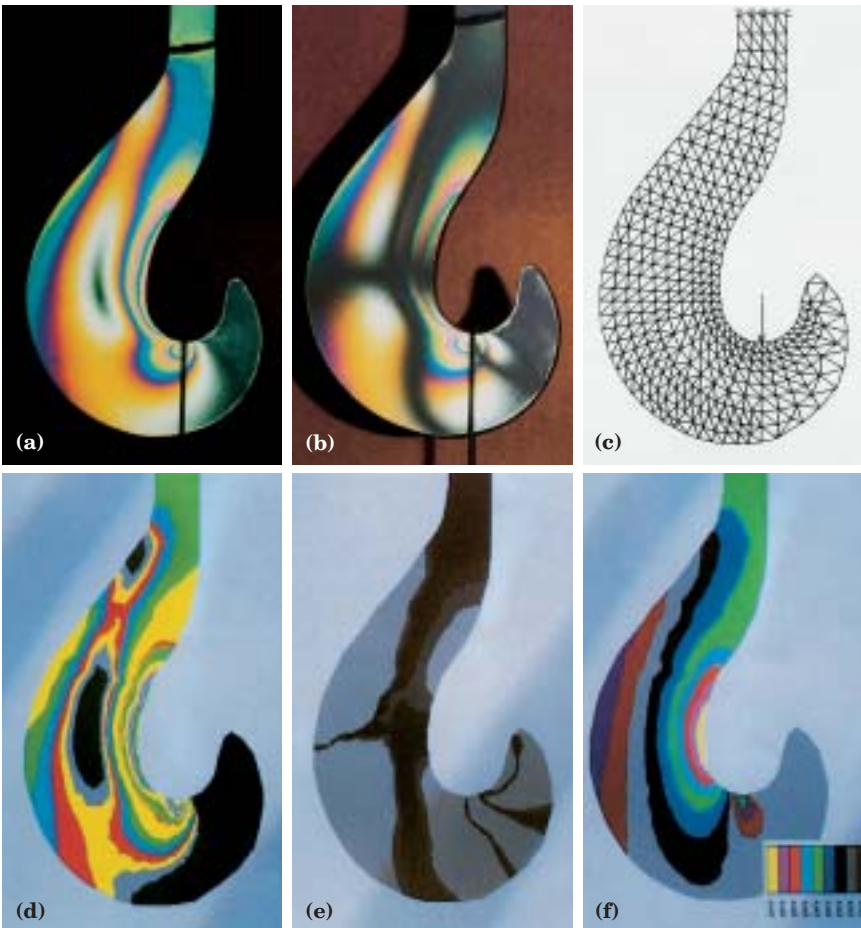


Fig. 59

*Coil Spring Support Bracket.* A more complex problem where PhotoStress was used to assist in the refinement of a finite-element model was in the design of an automotive coil spring support bracket. The stress distribution on the bracket as defined by FEA is shown in Fig. 60. It can be seen that the overall stress levels are low, with the absence of bright colors, and no significant stress concentrations are present. After manufacturing the initial prototype of the actual bracket, it was PhotoStress tested to verify the accuracy of the computer solution. The PhotoStress results showed a more complicated stress distribution than the finite-element model and revealed stress concentrations at specific locations on the bracket (Fig. 61). After witnessing how the spring loads were distributed to the bracket during the actual test (Fig. 62), it became clear that these load



Fig. 60

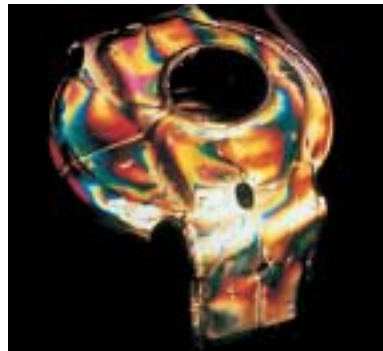


Fig. 61



Fig. 62



Fig. 63



inputs (spring expansion, compression, and variable bending) were not properly defined for the finite-element model. As a result of the PhotoStress analysis, the finite-element model was modified to more closely match the PhotoStress test results as shown in Fig. 63. Ongoing design changes were then incorporated into the bracket and more realistic finite element results were obtained with a better understanding of the load input distribution provided by PhotoStress testing.

*Steering Knuckle.* Another example described here is that of an FEA analysis of a steering knuckle. After manufacturing the actual part, PhotoStress testing was chosen to verify the FEA results. Figure 64a shows an illustration of the steering knuckle and how the directional loads were applied. Figure 64b shows the FEA results indicating that the highest stresses are located in the fillet area of the protruding spindle. Figure 64c shows a physical model of the actual part in the test rig for PhotoStress testing. Figure 64d shows the results of PhotoStress analysis confirming the general location of the significant stresses revealed on the FEA model. PhotoStress measurement however, showed that the peak stress magnitudes were approximately 20 percent higher than the computer solution.

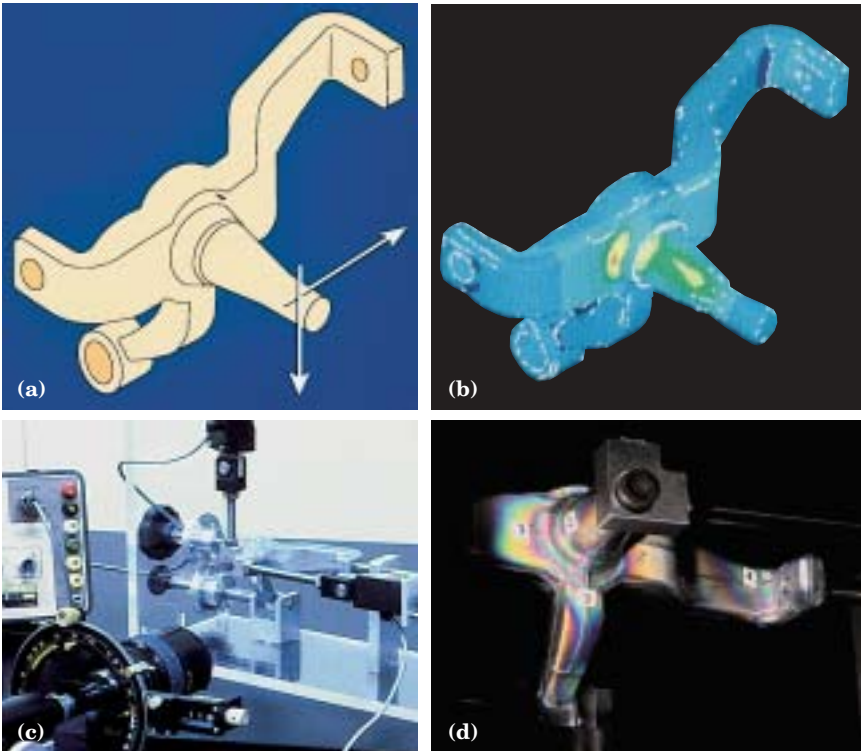


Fig. 64

## NOTES

## NOTES

## *The Americas*

**United States** **Vishay Precision Group – Micro-Measurements**  
P.O. Box 27777 • Raleigh, NC 27611  
Ph: +1-919-365-3800 • Fax: +1-919-365-3945  
E-mail: mm.us@vishaypg.com

## *Asia*

**P.R. China** **Vishay Precision Group – Micro-Measurements**  
A8220, Shanghai Jia Hua Business Center  
No. 808 Hong Qiao Road • Shanghai 200030  
Ph: +86-21-6448-6090, Ext. 6098 • Fax: +86-21-6448-6070  
E-mail: mm.cn@vishaypg.com

**Israel** **Vishay Precision Group – PhotoStress Technology**  
2 HaOfan Street • Holon 58814  
Ph: +972-3-557-0981 • +972-3-559-5715  
E-mail: photostress@vishaypg.com

## *Europe*

**France** **Vishay Precision Group – Micro-Measurements**  
16 Rue Francis Vovelle • 28000 Chartres  
Ph: +33-2-37-33-31-20 • Fax: +33-2-37-33-31-29  
E-mail: mm.fr@vishaypg.com

**Germany** **Vishay Precision Group – Micro-Measurements**  
Tatschenweg 1 • 74078 Heilbronn  
Ph: +49-7131-39099-0 • Fax +49-7131-39099-229  
E-mail: mm.de@vishaypg.com

**Spain** **Vishay Precision Group – Micro-Measurements**  
C/Copenhagen, N°4, 6 y 8 - Planta 1ª - Oficina 12 • Edificio Al Andalus  
Polígono Európolis • 28232 Las Rozas, Madrid  
Ph: +34-916-407-624 • Fax: +34-916-375-601  
E-mail: mm.es@vishaypg.com

**United Kingdom** **Vishay Precision Group – Micro-Measurements**  
Stroudley Road • Basingstoke • Hampshire RG24 8FW  
Ph: +44-(0)125-646-2131 • Fax: +44-(0)125-647-1441  
E-mail: mm.uk@vishaypg.com

© Copyright 2011 Vishay Precision Group. ® Registered trademarks of Vishay Precision Group. All rights reserved. Printed in USA. Specifications subject to change without notice.